JACS
JOURNAL OF THE AMERICAN CHEMICAL SOCIETY
Communication
pubs.acs.org/JACS

Selective Gas and Vapor Sorption and Magnetic Sensing by an Isoreticular Mixed-Metal–Organic Framework

Jesús Ferrando-Soria,[†] Pablo Serra-Crespo,[‡] Martijn de Lange,[‡] Jorge Gascon,*[,‡] Freek Kapteijn,[‡] Miguel Julve,[†] Joan Cano,[†] Francesc Lloret,*[,†] Jorge Pasán,[§] Catalina Ruiz-Pérez,[§] Yves Journaux,[∥] and Emilio Pardo*[,†]

[†]Departament de Química Inorgànica, Instituto de Ciencia Molecular (ICMOL), Universitat de València, 46980 Paterna, València, Spain

[‡]Catalysis Engineering-Chemical Engineering Department, Delft University of Technology, Julianalaan 136, 2628 BL Delft, The Netherlands

[§]Laboratorio de Rayos X y Materiales Moleculares, Departamento de Física Fundamental II, Universidad de la Laguna, E-38201 Tenerife, Spain

[∥]Institut Parisien de Chimie Moléculaire, Université Pierre et Marie Curie-Paris 6, UMR CNRS 7201, 75252 Paris cedex 05, France

Supporting Information

ABSTRACT: A novel isoreticular oxamato-based manganese(II)–copper(II) open metal–organic framework **H_2O@*iso*1** featuring a pillared square/octagonal layer structure with alternating open and closed octagonal pores has been rationally prepared. The open-framework topology is responsible for a large selectivity in the separation of small gas (CO_2 over CH_4) and vapor molecules (CH_3OH over CH_3CN and CH_3CH_2OH). **H_2O@*iso*1** displays a long-range three-dimensional ferromagnetic ordering with a drastic variation of the critical temperature as a function of the guest molecule [T_C < 2.0 K (**CO_2@*iso*1** and **CH_4@*iso*1**) and T_C = 6.5 (**CH_3OH@*iso*1**) and 21.0 K (**H_2O@*iso*1**)].

Multifunctional molecular materials[1] are currently a subject of intense research in materials science and nanotechnology because of the new potential applications that can be expected from them in very different fields.[2] The design and synthesis of molecule-based materials with tunable physical properties have largely benefited from the rapid development of extended coordination networks, the so-called metal–organic frameworks (MOFs).[3] These hybrid materials consist of metal ions (or small metal clusters) linked by a wide diversity of organic spacers.[4] MOFs presenting one or more functionalities in combination with their intrinsic porous open-framework structure offer new possibilities for applications in gas storage and separation, drug delivery, molecular recognition, and catalysis and as templates for nanoparticles and encapsulation of a wide variety of functional moieties.[5]

Among the variety of multifunctional MOFs reported to date, porous magnets, where the sorption properties coexist with a long-range magnetic ordering, have become one of the most challenging research fields for a great number of chemists, physicists, and materials scientists. The main goal in this intercrossing area of molecular magnetism and MOF chemistry is the modulation of the magnetic properties of the host open framework by the inclusion of selected guests such as solvents or gases through physi- or chemisorption processes, opening thus the way for future applications of porous magnets as magnetic sensors for host–guest molecular sensing.[6]

Our strategy to get porous magnets with predictable structures and tunable magnetic properties, which is based on the impressive and pioneering work of Kahn and co-workers,[7a] consists of using of ferromagnetically coupled, oxamato-based dinuclear M^{II}_2 metallacyclic complexes (M = Cu, Ni, Co) as ligands toward M'^{II} ions (M′ = Co, Mn) for the elaboration of mixed-metal–organic frameworks (M′MOFs).[7b−f] This metalloligand design strategy recently afforded a unique example of an oxamato-based three-dimensional (3D) M′MOF having the formula $[Na(H_2O)_4]_4\{Mn_4[Cu_2(mpba)_2(H_2O)_4]_3\}\cdot 56.5H_2O$ (**H_2O@1**) [$mpba^{4-}$ = *N*,*N*′-1,3-phenylenebis(oxamate)] and possessing a pillared square/octagonal layer structure (Scheme 1).[7b] **H_2O@1** exhibits reversible solvatomagnetic switching[1g,h] between high- and low-temperature ferromagnetically ordered states upon the complete loss of water to give the anhydrous derivative with the formula $Na_4\{Mn_4[Cu_2(mpba)_2]_3\}$ (**1**).

Scheme 1. Metalloligand Strategy for the Construction of 3D M′MOFs with a Pillared Square/Octagonal Structure (Right) Using Dinuclear Metallacyclophane Anions $[Cu^{II}_2L_2]^{4-}$ [L = mpba (X = H) and Me_3mpba (X = Me)] as Ligands toward Tris-chelated Mn^{II} Ions (Left)

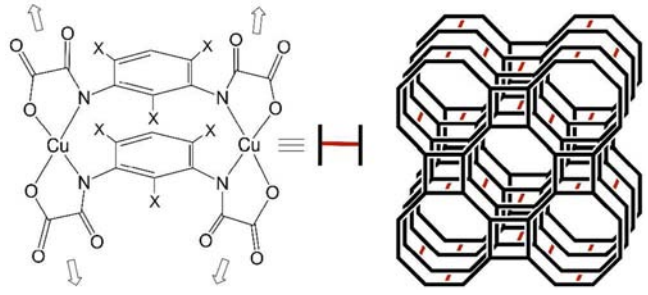

Received: May 11, 2012
Published: September 7, 2012

   dx.doi.org/10.1021/ja3045822 | *J. Am. Chem. Soc.* 2012, 134, 15301−15304

Herein we present the novel isoreticular analogue having the formula $[Na(H_2O)_{3.25}]_4\{Mn_4[Cu_2(Me_3mpba)_2(H_2O)_{3.33}]_3\}\cdot 37H_2O$ (**H_2O@*iso*1**) [Me_3mpba^{4-} = *N*,*N*′-2,4,6-trimethyl-1,3-phenylenebis(oxamate)]. Unlike the related compound **1**, the anhydrous derivative $Na_4\{Mn_4[Cu_2(Me_3mpba)_2]_3\}$ (***iso*1**) exhibits selective gas and vapor sorption behavior together with a drastic variation of the long-range magnetic properties as a function of the adsorbed guest, thus constituting the first example of a true 3D porous magnet within the class of oxamato-based M′MOFs.[7]

Like **H_2O@1**,[7b] **H_2O@*iso*1** crystallizes in the tetragonal $P4_2/mnm$ space group, but with very different unit cell dimensions that announce their distinct open-framework architectures. The most remarkable feature is the occurrence of an expansion of the unit cell along the *a* and *b* axes for **H_2O@*iso*1**, which leads to an overall increase in the unit cell volume of 1.7% with respect to that of **H_2O@1** [see the Supporting Information (SI)].

The 3D networks of **H_2O@*iso*1** and **H_2O@1** are topologically identical. They can be both described as an extended parallel array of anionic, oxamato-bridged $Mn^{II}_4Cu^{II}_6$ layers growing in the *ab* plane with a mixed square/octagonal ($4{\cdot}8^2$) net topology that are further interconnected through the two *m*-phenylene spacers among the Cu^{II} ions in an up-and-down disposition to yield a trinodal (3,4,4) net with a $(6^3)(6^4{\cdot}8^2)(6^4{\cdot}8{\cdot}10)$ topology (Figure 1).[7b] The resulting open-framework structure in **H_2O@*iso*1** presents a trimodal pore size distribution along the *c* axis (instead of a bimodal one as in **H_2O@1**) with small square pores and two types of large octagonal pores (Figure S1 in the SI). These two types of wide octagonal channels of **H_2O@*iso*1** (noted A and B in Figure 1) result from the distinct orientation of the trimethyl-substituted phenylene spacers pointing inward (A) or outward (B) of the channels. This situation is reflected both in their relative diameters of 1.5 (A) and 2.2 nm (B) and in their different occupation by the crystallization water molecules and the hydrated Na^+ countercations (Figure S2). Thus, the free H_2O molecules are unequally hosted within the hydrophobic (A) and hydrophilic (B) channels, whereas the tetraaquosodium ions are weakly bound to the carboxylate and carbonyl oxygen atoms from the oxamato groups within the B channels (Figure S2). The estimated empty volume without the crystallization water molecules is 11 997 Å^3, a value which represents up to ca. 60% of the potential void space per unit cell volume [V = 20 075 Å^3] (Figure S1a). Although the percentage of potential void space per unit cell volume is higher for **H_2O@1** (70%),[7b] **H_2O@*iso*1** presents two clear differences that can have influence on the adsorptive properties: (*i*) larger diameters for the octagonal pores as a consequence of the different orientation of the phenylene spacers, which is reflected in an increase in the accessible surface area of the MOF, and (*ii*) easier accessibility for the guest molecules to interact with the copper(II) ions within the B channels since the phenylene spacers pointing inward in the A channels (Figure S1).

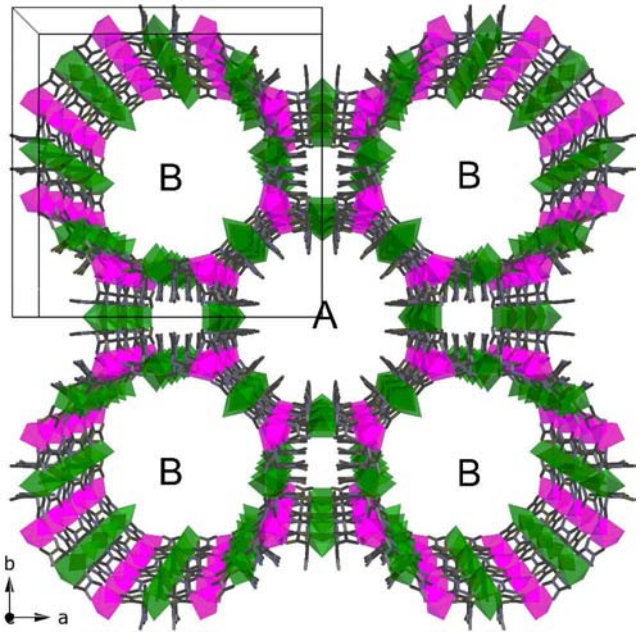

Figure 1. Perspective view of the 3D anionic network of **H_2O@*iso*1** along the crystallographic *c* axis showing the pillared square/octagonal layer architecture. Copper and manganese atoms are represented by green and purple octahedra respectively. Free water molecules and Na^+ counterions have been omitted for clarity.

The water content in **H_2O@*iso*1** was determined by thermogravimetric analysis (TGA) under a dry N_2 atmosphere. A fast mass loss from room temperature to ca. 125 °C was observed, followed by a plateau under further heating up to 250 °C, where decomposition started (Figure S3). The mass loss of ca. 30% at 125 °C corresponds to 60 H_2O molecules per formula unit, indicating that all of the water molecules were removed, resulting in the anhydrous compound ***iso*1**. Vapor adsorption/desorption isotherms for ***iso*1** showed a considerable adsorption of water (17.1 mol kg^{-1}) and methanol (10.4 mol kg^{-1}), corresponding to 60 (H_2O) and 37 (CH_3OH) molecules per formula unit (Figure S4). Under similar conditions, no vapor adsorption was observed for other solvents such as ethanol and acetonitrile. This fact indicates a large selectivity for the sorption of small molecules by ***iso*1** and suggests that both the kinetic diameter and the interaction with the network play key roles in the sorption process.

Because of the large selectivity of this system for small molecules and the growing interest in the development of energy-efficient methods for the separation of azeotropic mixtures, breakthrough experiments were performed in a column packed with ***iso*1**. The results obtained at 25 °C in the separation of an azeotropic CH_3CN/CH_3OH liquid mixture (79:21 v/v) are plotted in Figure 2. While CH_3CN eluted very rapidly from

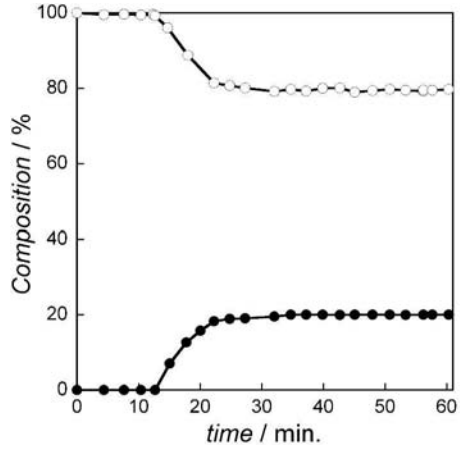

Figure 2. Evolution of the CH_3OH (●) and CH_3CN (○) concentrations after feeding of an azeotropic CH_3CN/CH_3OH liquid mixture (79:21 v/v) through a column packed with ***iso*1**.

dx.doi.org/10.1021/ja3045822 | *J. Am. Chem. Soc.* 2012, 134, 15301−15304

the column (retention time close to zero), CH_3OH was strongly retained (retention time of 12.70 min). In spite of the expected diffusion limitations, a sharp breakthrough was observed for methanol, and saturation of the adsorbent (9 mol kg^{-1}) was reached under dynamic conditions.

The accessible porosity of the anhydrous compound ***iso*1** was also estimated by means of gas adsorption isotherms at room temperature. CO_2 and CH_4 can enter the pores of ***iso*1** with loadings of 3.46 and 0.95 mol kg^{-1}, respectively, at 23 bar, which approximately correspond to 12.2 CO_2 and 3.3 CH_4 molecules per formula unit, respectively, indicating a moderate CO_2/CH_4 gas selectivity (the ideal selectivity is ca. 4; Figure S5). This situation clearly contrasts with that earlier found for **1**, where no gas or vapor sorption loadings were observed.[7b] This dramatically different sorption behavior can be attributed to the larger size of the channels present in ***iso*1** and/or the possible collapse of the structure in **1** upon removal of the solvent water molecules.[7b] Other gas molecules such as H_2 or N_2 were not adsorbed by ***iso*1** at room temperature, suggesting that they do not interact with the host network and thus confirming the large selectivity of this system for the separation of small molecules. We also measured the N_2 adsorption at 77 K to evaluate the surface area of ***iso*1** (Figure S6). As expected, hardly any N_2 uptake was observed at 77 K, demonstrating that adsorption of N_2 is highly diffusion-limited.

Depending on the nature of the guest molecule, four different adsorbates for ***iso*1** having the general formula $(Na)_4\{Mn_4[Cu_2(Me_3mpba)_2]_3\}\cdot mH_2O\cdot nCH_3OH\cdot pCO_2\cdot qCH_4$ ($m = 60$ and $n = p = q = 0$ for **H_2O@*iso*1**; $n = 37$ and $m = p = q = 0$ for **CH_3OH@*iso*1**; $p = 12$ and $m = n = q = 0$ for **CO_2@*iso*1**; $q = 3$ and $m = n = p = 0$ for **CH_4@*iso*1**) exist (Figure 3). Anhydrous

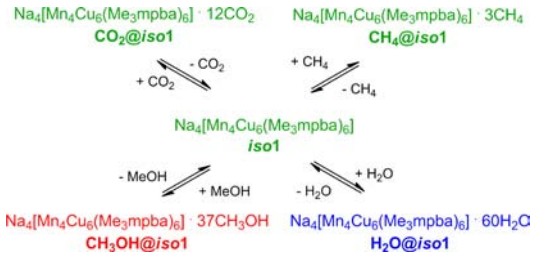

Figure 3. Synthetic route to the different adsorbates of ***iso*1**.

***iso*1** can easily be obtained by heating **H_2O@*iso*1** at 125 °C for 30 min under N_2. **H_2O@*iso*1** or **CH_3OH@*iso*1** can then be obtained by immersion of ***iso*1** in water or methanol, respectively, for 30 min. Alternatively, **CO_2@*iso*1** or **CH_4@*iso*1** can be obtained by introducing ***iso*1** into a sealed capillary tube filled with CO_2 or CH_4, respectively, at a pressure of 1 bar. To follow the structural changes between the different adsorbates of ***iso*1**, powder X-ray diffraction (PXRD) studies were carried out (Figure S7). The PXRD patterns showed an amorphization process when the as-synthesized **H_2O@*iso*1** was heated to get the anhydrous compound ***iso*1**, and therefore, no structural information on the activated species could be obtained. Interestingly, ***iso*1** recovered its crystallinity when immersed in water or methanol to give **H_2O@*iso*1** or **CH_3OH@*iso*1**, respectively, each of which presents the same 3D pillared square/octagonal layer structure.

Finally, we also studied the influence of the sorption of small molecules on the overall magnetic behavior. The plots of $\chi_M T$ versus T, where χ_M is the direct-current (dc) molar magnetic susceptibility per $Mn^{II}_4Cu^{II}_6$ unit and T is the temperature, exhibited characteristic minima at T_{min} = 125 (**H_2O@*iso*1**), 75 (**CH_3OH@*iso*1**), and 50 K (***iso*1**) (Figure S8a), which is indicative of 2D ferrimagnetic behavior resulting from the antiferromagnetic coupling between the high-spin Mn^{II} ($S_{Mn} = {}^5/_2$) and Cu^{II} ($S_{Cu} = {}^1/_2$) ions through the oxamato bridges.[7] The trend in the T_{min} values, ***iso*1** < **CH_3OH@*iso*1** < **H_2O@*iso*1**, thus indicates a weakening of the intralayer antiferromagnetic interactions along this series. The maximum magnetization (M) values of 12.50 (***iso*1**), 13.10 (**CH_3OH@*iso*1**), and 13.40 $N\beta$ (**H_2O@*iso*1**) at 5 T are consistent with the calculated values of the saturation magnetization for the antiparallel spin alignment of the high-spin Mn^{II} and Cu^{II} ions [$M_s = (4g_{Mn}S_{Mn} - 6g_{Cu}S_{Cu})N\beta = 13.7\ N\beta$ with $g_{Mn} = 2.0$ and $g_{Cu} = 2.1$][7b] (Figure S8b). However, the isothermal magnetization curve of **H_2O@*iso*1** exhibited very fast saturation, with ca. 95% of the maximum M value being reached at a field of 500 G, while those of ***iso*1** (and **CO_2@*iso*1**) did not saturate but showed a relatively small slope at low field values. The isothermal magnetization curve of **CH_3OH@*iso*1** showed intermediate behavior, reaching ca. 95% of the maximum M value at a field value of 2 T.

In fact, a paramagnetic to ferromagnetic phase transition is anticipated for ***iso*1** at a critical temperature (T_C) below 2.0 K, as revealed by the M versus T and χ''_M versus T plots, where χ''_M is the out-of-phase alternating-current (ac) molar magnetic susceptibility per $Mn^{II}_4Cu^{II}_6$ unit (Figure 4). This incipient long-range

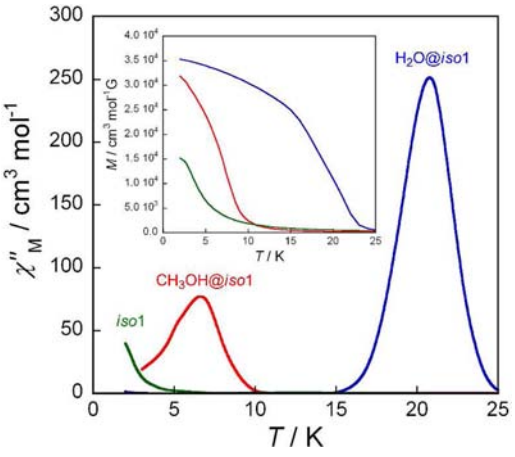

Figure 4. Temperature dependence of the out-of-phase molar ac magnetic susceptibility (χ''_M) of ***iso*1** (green), **CH_3OH@*iso*1** (red), and **H_2O@*iso*1** (blue) with a ±4.0 G field oscillating at 1000 Hz. The inset shows the temperature dependence of the magnetization (M) of the three adsorbates.

3D magnetic ordering is consistent with the occurrence of an effective interlayer ferromagnetic interaction resulting from the weak ferromagnetic coupling between the Cu^{II} ions across the double 2,4,6-trimethylphenylenebis(amidate) bridges within the dinuclear metallacyclophane pillaring units.[7b] Interestingly, the magnetic ordering temperature remained below 2.0 K for both **CO_2@*iso*1** and **CH_4@*iso*1** (data not shown) but progressively shifted to higher values for **CH_3OH@*iso*1** and **H_2O@*iso*1**, following the trend ***iso*1** < **CH_3OH@*iso*1** < **H_2O@*iso*1** ($T_c \approx 2.0$ K for ***iso*1**, **CO_2@*iso*1**, and **CH_4@*iso*1**; 6.5 K for **CH_3OH@*iso*1**; and 21 K for **H_2O@*iso*1**), as evidenced by the frequency-independent maximum in the χ''_M versus T plots (Figure 4). The observed variation in the magnetic behavior for the different adsorbates of ***iso*1** was repeated for several cycles of solvent adsorption/desorption with identical results. Hence, complete

dx.doi.org/10.1021/ja3045822 | J. Am. Chem. Soc. 2012, 134, 15301−15304

recovery of the long-range 3D ferromagnetic ordering was observed after the corresponding treatment of ***iso*1** to give **CH_3OH@*iso*1** and **H_2O@*iso*1**, thus supporting the reversible nature of the adsorption/desorption processes and the fast interconversion between the different adsorbates of ***iso*1**. The differences observed in the magnetic properties of **CH_3OH@*iso*1** and **H_2O@*iso*1** in comparison with ***iso*1** are likely related to the binding and removal of the axial solvent molecules (H_2O or CH_3OH) from the first coordination sphere of the Cu^{II} ion, as shown earlier for **1**.[7b] On the contrary, the fact that the magnetic properties of **CO_2@*iso*1** and **CH_4@*iso*1** are identical to those of ***iso*1** indicates that the adsorbed gas molecules do not appreciably interact with the magnetic host network.

In summary, a novel isoreticular oxamato-based mixed-metal−organic framework, ***iso*1**, was rationally prepared from the molecular-programmed self-assembly of permethylated dicopper(II) metallacyclophanes and Mn^{II} ions. Unlike its ancestor **1**, the coexistence of selective vapor and gas sorption behavior and solvent-dependent enhancement of the long-range magnetic ordering temperature offers fascinating possibilities in magnetic sensing of small guest molecules for this new member of the class of porous magnets.[8]

■ ASSOCIATED CONTENT

Ⓢ Supporting Information

Preparation and analytical and spectroscopic characterization of **H_2O@*iso*1**, X-ray data in CIF format, and Figures S1−S9. This material is available free of charge via the Internet at http://pubs.acs.org.

■ AUTHOR INFORMATION

Corresponding Author

j.gascon@tudelft.nl; francisco.lloret@uv.es; emilio.pardo@uv.es

Notes

The authors declare no competing financial interest.

■ ACKNOWLEDGMENTS

This work was supported by the MICINN (Spain) (Projects CTQ2010-15364, MAT2010-16981, CSD2007-00010, and DPI2010-21103-C04-03), the University of Valencia (Spain) (Project UV-INV-AE11-38904), the Generalitat Valenciana (Spain) (Projects PROMETEO/2009/108, GV/2012/051, and ISIC/2012/002), the ACIISI-Gobierno Autónomo de Canarias (Spain) (Project PIL-2070901), the ESRF (France) (Projects HS3902 and 25-01-783), and the MFR and the CNRS (France). We acknowledge the staff in charge of the BM16-CRG and BM25-CRG beamlines for their assistance and help in data collection. J.F.-S. thanks the Generalitat Valenciana for a doctoral grant. E.P. and J.P. thank the "Juan de la Cierva" (MICINN) and NANOMAC Projects (ACIISI-Gobierno Autónomo de Canarias), respectively, for contracts. J.G. gratefully acknowledges the Dutch National Science Foundation (NWO-CW- VENI) for financial support.

■ REFERENCES

(1) (a) Sato, O. *Acc. Chem. Res.* **2003**, *36*, 9692. (b) Nuida, T.; Matsuda, T.; Tokoro, H.; Sakurai, S.; Hashimoto, K.; Ohkoshi, S. *J. Am. Chem. Soc.* **2005**, *127*, 11604. (c) Long, J. R.; Yaghi, O. M. *Chem. Soc. Rev.* **2009**, *38*, 1213. (d) Train, C.; Gheorghe, R.; Krstic, V.; Chamoreau, L. M.; Ovanesyan, N. S.; Rikken, G. L. J. A.; Gruselle, M.; Verdaguer, M. *Nat. Mater.* **2008**, *9*, 729. (e) Ohkoshi, S.; Arai, K.; Sato, Y.; Hashimoto, K. *Nat. Mater.* **2004**, *3*, 857. (f) Pardo, E.; Train, C.; Gontard, G.; Boubekeur, K.; Fabelo, O.; Liu, H.; Dkhil, B.; Lloret, F.; Nakagawa, K.; Tokoro, H.; Ohkoshi, S. I.; Verdaguer, M. *J. Am. Chem. Soc.* **2011**, *133*, 15328. (g) Maspoch, D.; Ruiz-Molina, D.; Wurst, K.; Domingo, N.; Cavallini, M.; Biscarini, F.; Tejada, J.; Rovira, C.; Veciana, J. *Nat. Mater.* **2003**, *2*, 190. (h) Kahn, O.; Larianova, J.; Yakhmi, J. V. *Chem.—Eur. J.* **1999**, *5*, 3443.

(2) Turnbull, M. M.; Sugimoto, T.; Thompson, L. K. *Molecule-Based Magnetic Materials*; American Chemical Society: Washington, DC, 1996.

(3) (a) Batten, S. R.; Robson, R. *Angew. Chem., Int. Ed.* **1998**, *37*, 1460. (b) Janiak, C. *Dalton Trans.* **2003**, 2781. (c) Dechambenoit, P.; Long, J. R. *Chem. Soc. Rev.* **2011**, *40*, 3249. (d) Das, M. C.; Xiang, S.; Zhang, Z.; Chen, B. *Angew. Chem., Int. Ed.* **2011**, *50*, 10510. (e) Xiang, S.-C.; Zhang, Z.; Zhao, C.-G.; Hong, K.; Zhao, X.; Ding, D.-R.; Xie, M.-H.; Wu, C.-D.; Das, M. C.; Gill, R.; Thomas, K. M.; Chen, B. *Nat. Commun.* **2011**, *2*, 204. (f) Chen, B.; Zhao, X.; Putkham, A.; Hong, K.; Lobkovsky, E. B.; Hurtado, E. J.; Fletcher, A. J.; Thomas, K. M. *J. Am. Chem. Soc.* **2008**, *130*, 6411. (g) Kreno, L. E.; Leong, K.; Farha, O. K.; Allendorf, M.; Van Duyne, R. P.; Hupp, J. T. *Chem. Rev.* **2012**, *112*, 1105. (h) Farha, O. K.; Hupp, J. T. *Acc. Chem. Res.* **2010**, *43*, 1166. (i) Lu, G.; Hupp, J. T. *J. Am. Chem. Soc.* **2010**, *132*, 7832.

(4) (a) Eddaoudi, M.; Kim, J.; Rosi, N.; Vodak, D.; Watcher, J.; O'Keeffe, M.; Yaghi, O. M. *Science* **2002**, *295*, 469. (b) Rosi, N.; Eckert, J.; Eddaoudi, M.; Vodak, D.; Kim, J.; O'Keeffe, M.; Yaghi, O. M. *Science* **2003**, *300*, 1127. (c) Zhao, D.; Timmons, D. J.; Yuan, D. Q.; Zhou, H. C. *Acc. Chem. Res.* **2011**, *44*, 123.

(5) (a) Yaghi, O. M.; O'Keeffe, M.; Eddaoudi, M.; Chae, H. K.; Kim, J.; Ockwig, N. W. *Nature* **2003**, *423*, 705. (b) Kitagawa, S.; Kitaura, R.; Noro, S.-I. *Angew. Chem., Int. Ed.* **2004**, *43*, 2334. (c) Maspoch, D.; Ruiz-Molina, D.; Veciana, J. *Chem. Soc. Rev.* **2007**, *36*, 770. (d) Férey, G. *Chem. Soc. Rev.* **2008**, *37*, 191. (e) Kuppler, R. J.; Timmons, D. J.; Fang, Q.-R.; Li, J.-R.; Makal, T. A.; Young, M. D.; Yuan, D.; Zhao, D.; Zhuang, W.; Zhou, H.-C. *Coord. Chem. Rev.* **2009**, *253*, 3042. (f) Chen, B.; Xiang, S.; Qian, G. *Acc. Chem. Res.* **2010**, *43*, 1115. (g) Li, J.-R.; Sculley, J.; Zhou, H.-C. *Chem. Rev.* **2012**, *112*, 869. (h) Juan-Alcañiz, J.; Gascon, J.; Kapteijn, F. *J. Mater. Chem.* **2012**, *22*, 10102. (i) Ferrando-Soria, J.; Khajavi, H.; Serra-Crespo, P.; Gascon, J.; Kapteijn, F.; Julve, M.; Lloret, F.; Ruiz-Pérez, C.; Journaux, Y.; Pardo, E. *Adv. Mater.* **2012**, DOI: 10.1002/adma.201201846.

(6) (a) Pardo, E.; Ruiz-García, R.; Cano, J.; Ottenwaelder, X.; Lescouëzec, R.; Journaux, Y.; Lloret, F.; Julve, M. *Dalton Trans.* **2008**, 2780. (b) Kurmoo, M. *Chem. Soc. Rev.* **2009**, *38*, 1353. (c) Dul, M.-C.; Pardo, E.; Lescouëzec, R.; Journaux, Y.; Ferrando-Soria, J.; Ruiz-García, R.; Cano, J.; Julve, M.; Lloret, F.; Cangussu, D.; Pereira, C. L. M.; Stumpf, H. O.; Pasán, J.; Ruiz-Pérez, C. *Coord. Chem. Rev.* **2010**, *254*, 2281. (d) Dechambenoit, P.; Long, J. R. *Chem. Soc. Rev.* **2011**, *40*, 3249.

(7) (a) Stumpf, H. O.; Ouahab, L.; Pei, Y.; Grandjean, D.; Kahn, O. *Science* **1993**, *261*, 447. (b) Ferrando-Soria, J.; Ruiz-García, R.; Cano, J.; Stiriba, S.-E.; Vallejo, J.; Castro, I.; Julve, M.; Lloret, F.; Amorós, P.; Pasán, J.; Ruiz-Pérez, C.; Journaux, Y.; Pardo, E. *Chem.—Eur. J.* **2012**, *18*, 1608. (c) Pardo, E.; Cangussu, D.; Dul, M.-C.; Lescouëzec, R.; Herson, P.; Journaux, Y.; Pedroso, E. F.; Pereira, C. L. M.; Muñoz, M. C.; Ruiz-García, R.; Cano, J.; Amorós, P.; Julve, M.; Lloret, F. *Angew. Chem., Int. Ed.* **2008**, *47*, 4211. (d) Cangussu, D.; Pardo, E.; Dul, M. C.; Lescouëzec, R.; Herson, P.; Journaux, Y.; Pedroso, E. F.; Pereira, C. L. M.; Stumpf, H. O.; Muñoz, M. C.; Ruiz-García, R.; Cano, J.; Julve, M.; Lloret, F. *Inorg. Chim. Acta* **2008**, *361*, 3394. (e) Ferrando-Soria, J.; Pasán, J.; Ruiz-Pérez, C.; Journaux, Y.; Julve, M.; Lloret, F.; Cano, J.; Pardo, E. *Inorg. Chem.* **2011**, *50*, 8694. (f) Pereira, C. L. M.; Pedroso, E. F.; Stumpf, H. O.; Novak, M. A.; Ricard, L.; Ruiz-García, R.; Rivière, E.; Journaux, Y. *Angew. Chem., Int. Ed.* **2004**, *43*, 956.

(8) (a) Ohba, M.; Yoneda, K.; Agustí, G.; Muñoz, M. C.; Gaspar, A. B.; Real, J. A.; Yamasaki, M.; Ando, H.; Nakao, Y.; Sasaki, S.; Kitagawa, S. *Angew. Chem., Int. Ed.* **2009**, *48*, 4652. (b) Jiang, H.-L.; Tatsu, Y.; Lu, Z.-H.; Xu, Q. *J. Am. Chem. Soc.* **2010**, *132*, 5586. (c) Takashima, Y.; Martínez, V. M.; Furukawa, S.; Kondo, M.; Shimomura, S.; Uehara, H.; Nakahama, M.; Sugimoto, K.; Kitagawa, S. *Nat. Commun.* **2011**, *2*, 168.